

International Journal of Heat and Technology

Vol. 43, No. 5, October, 2025, pp. 1703-1710

Journal homepage: http://iieta.org/journals/ijht

Investigating the Impact of Porous Glass Balls of Various Diameters on Heat Transfer Coefficient in a Vertical Channel



Furqan Haider Mohammed Ali[®], Intisar Khalaf[®], Zhala Azeez Mohammed[®], Ehsan Fadhil Abbas[®], Hussein Hayder Mohammed Ali[®]

Engineering Technical College, Kirkuk – Northern Technical University, Kirkuk 3006, Iraq

Corresponding Author Email: ehsanfadhil@ntu.edu.Iq

Copyright: ©2025 The authors. This article is published by IIETA and is licensed under the CC BY 4.0 license (http://creativecommons.org/licenses/by/4.0/).

https://doi.org/10.18280/ijht.430509

Received: 28 July 2025 Revised: 11 September 2025 Accepted: 23 September 2025 Available online: 31 October 2025

Keywords:

free convection, porosity, glass balls, flow in vertical channel, heat flux, porous pad

ABSTRACT

This study examines the effect of porous glass ball diameter on free convection heat transfer in a vertical channel. Three diameters (11.4, 15.6, and 20 mm) were tested in a 15 \times 13 \times 60 cm duct with electric heaters, under heat fluxes of 530–2100 W/m² for a single heated plate and double for two plates. Air mass flow rate, heat transfer coefficient, and pressure drop were evaluated. Results show that the 20 mm balls delivered the best thermal performance, with air mass flow rates 83.5% and 11.6% higher than those for 11.4 and 15.6 mm balls, respectively. They also produced the lowest pressure drop, while the smallest balls caused the highest, increasing by 33.6% and 45% relative to 15.6 and 20 mm balls. These findings highlight the significant influence of porous media size on enhancing heat transfer while minimizing flow resistance. The achieved results agree with previous studies in similar fields.

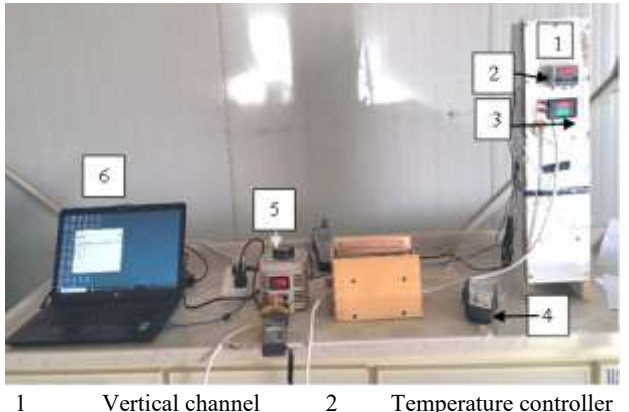
1. INTRODUCTION

Heat exchangers are essential thermal devices designed to facilitate the transfer of thermal energy between two or more fluids. Typically, these systems employ a solid wall to prevent mixing of the fluids while allowing efficient heat transfer. They are integral to various industrial processes such as those in power plants, refrigeration systems, chemical processing, nuclear facilities, and dairy production [1]. Given the growing global demand for energy and the increasing emphasis on its efficient use, researchers have focused on enhancing energy production efficiency and minimizing energy losses. One of the key strategies to achieve this is through the improvement of heat transfer rates while minimizing heat dissipation within heat exchangers. A promising passive approach to this enhancement involves the use of porous materials within the fluid flow system [2]. Pavel and Mohamad [3] studied the impact of porous metal inserts on heat transfer in a heated tube. Using a constant heat flux, they examined porosity, material diameter, thermal conductivity, and Reynolds number with respect to heat transfer and pressure drop. They found that porous inserts enhanced heat transfer but also increased pressure drop, and emphasized the need for accurate modeling of effective thermal conductivity in such systems. Dehghan et al. [4] analyzed heat transfer enhancement and pressure drop in microchannels with porous inserts. Using the Darcy-Brinkman and binary energy equations under local thermal non-equilibrium, they showed that rarefied porous inserts in the sliding flow regime $(0.001 \le \text{Kn} \le 0.1)$ markedly improved heat transfer, offering potential for compact, low-cost heat exchanger design. Mahmoudi and Maerefat [5] analytically studied heat transfer in a channel partially filled with porous material under local thermal non-equilibrium. They derived exact temperature profiles for the fluid and solid phases, accounting for insert thickness, porosity, conductivity ratio, Biot number, and Darcy number. Results showed that optimal insert thickness improves heat transfer and varies linearly with the Darcy number. Mohammadi and Karimi [6] numerically examined heat transfer in a tube partially filled with porous material under local thermal non-equilibrium. Using the Darcy-Brinkman-Forchheimer model, they evaluated the effects of porosity, particle diameter, and inertia. They identified an optimal porous layer thickness that enhances heat transfer while limiting pressure drop and showed that the inertia term significantly influences performance at higher Reynolds numbers. In a theoretical investigation, Mohamad [7] examined the impact of fixed-wall temperature porous media on heat transfer in tubes partially filled with porous materials. Their study hypothesized forced laminar flow conditions and investigated the effects of porous layer thickness and Darcy number on heat transfer rates. They concluded that partial filling of the channel with a porous medium improved heat transfer efficiency while reducing pressure drop, particularly for Darcy numbers lower than 10⁻³. Wang et al. [8] introduced a graded porous material (GPM) in tubes to improve heat transfer and reduce fluid flow resistance. Their study compared GPM with non-porous homogeneous porous materials, demonstrating that GPM configurations enhanced heat transfer while maintaining low friction. They employed field synergy theory to explain the heat transfer mechanisms and performed a trade-off analysis between pressure reduction and improved heat transfer. Yousif et al. [9] conducted both practical and theoretical investigations to assess the effects of porous materials on heat transfer in concentric vertical annular tubes. The study, using numerical simulation, explored a range of Reynolds numbers and porosity sizes, revealing that the Nusselt number increased as porosity decreased, with the highest heat transfer occurring at lower porosities. Abdulkareem and Hilal [10] carried out an experimental study on heat transfer in a porous vertical channel, examining the effects of different diameters of glass beads. The results showed that heat transfer improved as bead diameter increased from 1 mm to 3 mm, but decreased with a further increase in diameter. The study also noted that pressure loss increased with higher porosity. In another study, Yousif [11] examined forced convection through porous vertical rings, finding that increasing particle size and decreasing porosity led to significant improvements in thermal performance. Their experimental results showed that the Nusselt number for vertical porous rings was up to three and a half times greater than for rings without porous material. Abbas [12] studied the flow of fluids through a packed spherical column, comparing different packing materials and porosities. The study found that the modified porosity equation provided results that closely aligned with experimental data, offering an accurate model for predicting fluid flow through packed media. Saleh [13] investigated convective heat transfer in channels of various cross-sections filled with porous materials. His study showed that as the Reynolds number increased, the Nusselt number improved, with the triangular channel exhibiting better thermal performance than rectangular or cylindrical channels. Yang et al. [14] conducted a numerical simulation of heat transfer in porous media at high porosity. They observed that while increasing Reynolds and rotation numbers enhanced the Nusselt number, increasing porosity led to a gradual decrease in heat transfer efficiency. Yuan et al. [15] investigated heat transfer and friction characteristics in turbulent flow through a circular tube equipped with spherical impellers. Their study revealed that smaller ball diameter ratios and shorter spacing lengths were more effective in enhancing heat transfer and reducing friction. Hilal et al. [16] performed experiments on heat transfer in porous heat exchangers with a rectangular channel, noting significant increases in Nusselt numbers at higher Reynolds numbers and heat fluxes. They found that porosity had a substantial impact on heat transfer performance. Jiang et al. [17] studied the forced convection of water and air in channels with sintered porous plates. They found that sintered porous materials significantly improved heat transfer compared to uncentered plates, particularly at higher flow rates and with lower porosity near the wall. Zhang et al. [18] investigated a lotus-type porous copper heat sink and demonstrated excellent heat transfer performance, highlighting the importance of optimizing porosity and pore penetration for improved heat transfer in porous media heat exchangers. Rashid and Hassan [19] studied natural convection from a heated triangular copper prism in a porous medium. Using a packed vertical channel, they found that the base-down orientation produced higher surface temperatures, while the base-up orientation achieved better heat transfer, with empirical correlations closely matching experimental results (±0.2% error). Hassan et al. [20] examined turbulent forced convection in a cylindrical porous channel with internal heat generation. The setup used steel balls heated by electromagnetic induction, with dry air as the coolant, in a 500 mm \times 47 mm copper test section. Tests (Re = 490–5490) assessed ball diameter, porosity, and velocity. A 6% porosity reduction increased heat transfer by 38% (Re = 750-3000). Higher Reynolds numbers and heat generation boosted Nusselt numbers by 20% but raised pressure drop by 200%. Salman et al. [21] investigated PV module cooling using a porous medium with water circulation in a back chamber. ANSYS simulations and experiments evaluated flow rate, solar intensity, and porosity effects. The porous medium lowered PV temperatures by 9–14°C, with higher flow rates improving cooling. Experimental results closely matched simulations, confirming the method's effectiveness for PV thermal management. Mahdi and Rashid [22] experimentally investigated convective heat transfer in a triangular channel filled with porous media under a constant heat flux of 1300 W/m². The 1 m-long channel, with a 0.1 m hydraulic diameter, was packed with 5 mm and 10 mm glass spheres, resulting in porosities of 0.616 and 0.468. Experiments over a Reynolds number range of 3165-10910 showed that porous media enhanced the convective heat transfer coefficient by 90.2% and 92.1% compared to an empty channel. Higher air velocity decreased the local Nusselt number axially, increased end pressures, and lowered drag with larger particles. Ali and Rashid [23] experimentally studied forced convection in a square channel partially filled with glass spheres (5 mm) under constant heat flux. Porous media heights of 20-60 mm were tested with Re = 2,690-5,806. Results showed notable heat transfer enhancement, especially at 60 mm. Higher Reynolds numbers reduced wall temperature and increased Nusselt number, while friction factor decreased with velocity, improving overall thermo-hydraulic performance. Boulhidja et al. [24] numerically investigated an inclined PV/T solar collector with an integrated porous medium under mixed convection. The study assessed panel tilt, Richardson number, porous layer thickness, and Darcy number. Results showed that a porous medium with intermediate permeability could improve thermal and electrical efficiencies by over 28% under optimal conditions, demonstrating its potential for PV/T performance enhancement. Saihood and Ala [25] studied natural convection in a porous cavity partially open to air, filled with glass beads. Varying heat fluxes and open side ratios, they found that higher heat flux and smaller openings enhanced heat transfer, increasing the local Nusselt number by up to 5.47% and the average Nusselt number by up to 7.28%. Xiang et al. [26] examined flow and heat transfer in singletube liquid-solid fluidized bed heat exchangers. Experiments showed that higher fluid flow rates and smaller particle sizes improved heat transfer efficiency, providing guidance for optimizing the design and operation of these heat exchangers in industrial applications. Bavandla and Srinivasan [27] experimentally studied Rayleigh-Bénard convection in gassaturated porous media at very low Darcy numbers (5.87 × $10^{-8} - 1.94 \times 10^{-6}$). Heat transfer increased linearly just beyond onset, with divergence at higher modified Rayleigh numbers depending on Darcy number. Large pores exhibited behavior similar to classical convection, though Brinkman drag remained significant. Karra and Apte [28] used large-eddy simulation with a variable-porosity continuum model to study turbulent open-channel flow over a randomly packed sediment bed. At Re_k \approx 2.56 and Re τ = 270, the smoothly varying porosity and modified Ergun-Forchheimer drag captured mean flow, Reynolds stresses, and momentum exchange in good agreement with pore-resolved DNS, while significantly reducing computational cost for large-scale aquatic flow studies. Lee et al. [29] experimentally examined heat transfer in porous media to test local thermal equilibrium (LTE) under different grain sizes and flow velocities. Using 5-30 mm glass spheres and Darcy velocities of 3-23 m/d, they found stronger local thermal non-equilibrium (LTNE) effects with larger grains and higher velocities. LTE/LTNE models matched data for small grains but failed for 20-30 mm, where phase temperature differences exceeded 5% of the gradient. The onedimensional LTNE model could not capture non-uniform flow, highlighting the need for multidimensional modeling in coarse-grained systems such as gravel aquifers. Bansal [30] studied heat transfer enhancement in fluidized-bed reactors using 600 µm iron oxide-coated glass beads. Experiments (BET, XRD, SEM) assessed coating quality, while air velocity, heating power, surface area, and thermal conductivity were evaluated for their impact on heat transfer. A random forest model accurately predicted performance, optimized conditions reaching 390.3 W/m²·kg, with demonstrating that nanoscale coatings combined with machine learning can effectively enhance thermal performance in gassolid fluidized beds. Singh et al. [31] experimentally studied heat transfer in a solid-fluidized bed, examining particle size and fluid type (water, sodium carboxymethylcellulose). They found that higher particle size and interfacial fluid velocity increased the bed void fraction (ϵ) and heat transfer coefficient (h), which peaked at $\epsilon \approx 0.7$. Fluidization regimes varied with fluid concentration, and nonuniform radial temperature profiles indicated significant bulk resistance affecting overall heat transfer. Zhang et al. [32] developed a porous glass bead photoreactor (APR) with zirconia for Rhodamine B degradation in wastewater. Under optimal conditions (120 mL/min flow, 13 mm liquid layer), over 99% removal was achieved in 9 hours, following a diffusion-controlled first-order kinetic model ($k = 0.55 h^{-1}$). Simulations showed that microarray particles enhanced local flow (0.25 m/s), improving performance, demonstrating APR's potential for efficient photocatalytic wastewater treatment. Zhang et al. [33] studied steady-state porosity in fluidized beds at low Reynolds numbers using experiments and numerical simulations. Upward flow of spherical particles was visualized in a transparent permeameter, and porosity was measured via image-based aggregate thickness. CFD-DEM simulations with various drag models matched experimental and analytical results, validating the approach and improving understanding of low-Re fluidized-bed behavior relevant to internal corrosion analysis. Sheppard et al. [34] investigated freeze-casting laminar porous copper from cupric oxide suspensions to enhance transverse thermal conductivity. Controlled freezing, sublimation, reduction, and sintering produced laminates with porosity 66.7-89.5% and conductivity 9.5-12.9 W/m·K; the highest conductivity (16.7 W/m·K) occurred at 65.7% porosity and 13 vol% particle loading. Cooling rates and PVA content influenced laminate formation, porosity, and conductivity, with freeze-cast copper outperforming commercial foams. Hilal et al. [35] experimentally studied forced convection in an inclined square porous duct filled with high-porosity (~0.99) zig-zag metallic mesh. Tests (Re = 8,355-18,600; heat flux = $480-1,520 \text{ W/m}^2$; angles 30°-60°) showed that higher Reynolds number, heat flux, and inclination increased local and average Nusselt numbers, with up to 24% enhancement at 60° compared to horizontal. Saqar et al. [36] a double-pass solar air heater (DPSAH) integrated with two types of porous media and a fin plate was experimentally evaluated under forced convection. The objective was to enhance heat transfer and storage efficiency. Methodology involved performance testing under varying airflow conditions. Findings revealed a 2-5% efficiency improvement and higher outlet temperatures compared to conventional systems.

Previous studies on heat transfer in porous media used analytical, numerical, and experimental methods to examine various geometries (tubes, ducts, channels) and porous fillings such as foams, packed beds, and coated beads. Conducted under forced and natural convection and local thermal nonequilibrium, most highlighted the trade-off between heat transfer enhancement and pressure drop. Strategies like gradient porous designs, microchannels, and variable porosity sought to optimize performance. However, limited work has experimentally isolated structural effects. This study addresses that gap by examining porous ball diameter variation (11.4–20 mm) under free convection, quantifying its impact on heat transfer and flow resistance.

2. EXPERIMENTAL SETUP

The experimental setup, as depicted in Figure 1, comprises three primary components. The first component is a vertical channel constructed from an MDF panel with dimensions of $15 \times 13 \times 60$ cm. Two heating plates, each measuring 13×20 cm, are positioned symmetrically at the midpoint of the channel, with one on each parallel side. Each heating plate is equipped with a 200 W electric element, characterized by an electrical resistance of 242 Ω . The second component is the power supply, which consists of a variac device rated at 1000 VA. This device regulates the power delivered to the electric elements. The third component includes several measurement instruments: A voltmeter and an ammeter to measure the electric power supply, a temperature controller to set the temperature of the heating surfaces, a hot-wire manometer to measure pressure drop across the porous pad and air velocity exiting the channel, and temperature data loggers to record the temperature within the experimental space. Three distinct porous pads, each containing glass balls with identical volumes, were utilized: the first pad contained 3.39 kg of 11.4 mm diameter glass balls, the second contained 4.05 kg of 15.6 mm diameter glass balls, and the third contained 3.685 kg of 20 mm diameter glass balls. The details of these samples' scaling are shown in Figure 2. The experiments were carried out under two different ranges of heat flux. When heating a single side of the plate, the heat flux varied from 530 to 2100 W/m², while heating both sides of the plate resulted in a heat flux range from 1060 to 4200 W/m².



- Vertical channel
 - 4 Power meter Variac transformer 6
- Temperature controller Hotwire anemometer PC computer

Figure 1. Photo of the test rig used

The porosity of the glass ball pad was measured in the laboratory using a three-step process. First, a specific number of glass balls was packed into a scaled cylinder (V_b). In the second step, the balls were fully submerged in water. Finally, the water that filled the space around the balls was poured into another scaled cylinder, and its volume was measured (V_w). Figure 3 shows the steps of porosity scaling practically. The porosity (ε) was calculated using the formula below, and the values can be found in Table 1:

$$\varepsilon = \frac{V_b - V_w}{V_h} \tag{1}$$







Figure 2. Photos of glass ball samples used, (A) 20 mm, (B) 15.6 mm, (C) 11.4 mm



Figure 3. Steps for determining the porosity of glass balls pad

Table 1. Practical scaling of porosity for various glass ball diameters

Ball Diameter (mm)	Weight (kg)	Porosity	Symbol
11.4	3.39	0.444	B1
15.6	4.05	0.5	B2
20	3.685	0.534	В3

The total power provided to heat the plate can be calculated as [10]:

$$P_{ele} = q_{in} = V \times I \tag{2}$$

The net heat transfer from the heated plate to the porous pad can be expressed as follows:

$$Q = q_{in} - (q_o + q_r) \tag{3}$$

The heat loss from the test rig structure is due to heat transfer by free convection and radiation from its outer surface to the surroundings. Both can be calculated using the following equations [37]:

Heat transfer by free convection is calculated as:

$$q_o = h_o A_o (T_s - T_\infty) \tag{4}$$

Heat transfer by radiation is calculated as:

$$q_r = \sigma \epsilon A_o (T_s^4 - T_\infty^4) \tag{5}$$

Thus, the convection heat transfer in the workspace is calculated based on Newton's cooling equation, as shown below:

$$Q = h_{av} A_p (\bar{T}_w - T_b) \tag{6}$$

and

$$h_{av} = \frac{Q}{A_p(\bar{T}_W - T_b)} \tag{7}$$

since

$$\bar{T}_{w} = \frac{1}{n} \sum_{i=1}^{n} T_{w,i}$$
 (8)

And

$$T_b = \frac{T_{in} + T_{out}}{2} \tag{9}$$

3. EXPERIMENTAL UNCERTAINTY ANALYSIS

To estimate the precision of the experimental results, the error rate of the mechanical or electrical measuring devices used in this study was calculated using the uncertainty Eq. (10) [39]. EES software was used to evaluate their uncertainty. The results are shown in Table 2. It has been found that the maximum heat flux and transfer coefficient uncertainty are approximately (4.176 and 1.646) W/m², respectively.

$$w_r = \left[\left(\frac{\partial r}{\partial x_1} w_1 \right)^2 + \left(\frac{\partial r}{\partial x_2} w_2 \right)^2 + \dots \left(\frac{\partial r}{\partial x_n} w_n \right)^2 \right]^{1/2} \tag{10}$$

Table 2. Uncertainty of the measuring devices used

Device Name	Resolution	Accuracy	Uncertanity
Temprature datalogger	0.5°C	±0.2%°C	±0.293°C
Voltmeter	0.1 V	$\pm 1.2\% \text{ V} + 3\text{ V}$	$\pm 1.2 V$
Ammeter	0.01A	$\pm 2.5A\% + 5A$	$\pm 0.02 A$
Air speed	0.001 m/s	$\pm 3\%$ m/s + 0.1 m/s	$\pm 0.03~m/s$

4. RESULTS and DISCUSSION

The experiments were conducted using three different diameters of glass ball pads under three heat fluxes ranging from 530 to 4200 W/m², employing a single heated plate and two parallel heated plates. The heating process within the working space induced accelerated air movement as a result of density variations, effectively transitioning the system from a free convection regime to a forced convection regime. This transition was confirmed by the observed increase in air mass flow rates. The results discussion encompasses the evaluation of mass flow rate, convective heat transfer coefficient, and pressure drop as functions of the Reynolds number, corresponding to the applied heat flux levels.

4.1 Mass flow rate

The results indicate that the mass flow rate is significantly

influenced by the diameter of the balls due to their impact on porosity. Larger spheres (B3) created wider flow passages, which reduced viscous resistance and allowed for higher airflow. In contrast, smaller spheres (B1) restricted flow because of lower porosity and higher tortuosity, even though they generated locally higher velocities. As illustrated in Figures 4 and 5, the mass flow rate increased with heat flux due to buoyancy-driven acceleration, confirming the transition from natural to forced convection. Under single-plate heating, B3 achieved the highest mass flow rates, ranging from 0.2107 to 0.2304 g/s. This was 59.2% higher than B1 and 37.2% higher than B2. When using two-plate heating, the effect of porosity was even more pronounced, with B3 reaching mass flow rates between 0.235 and 0.352 g/s. This represents an increase of 83.5% compared to B1 and 11.6% compared to B2, resulting in an overall increase of 46.1% compared to singleplate heating. These findings are consistent with those of Ahn et al. [40], who reported that larger pore sizes enhance natural convection by facilitating airflow and reducing flow resistance.

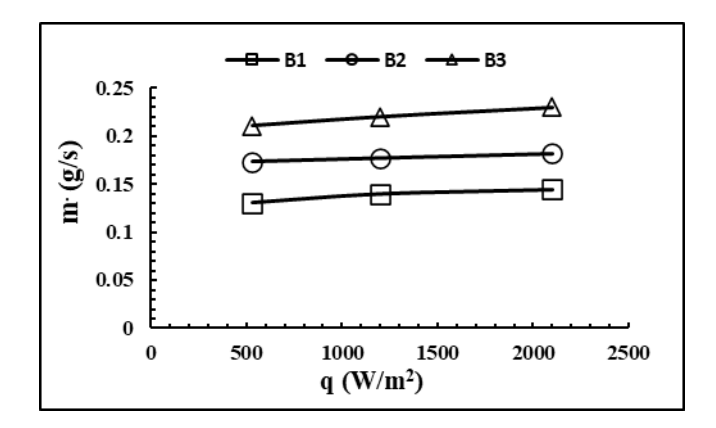


Figure 4. Variation of mass flow rate versus heat flux on single side of a heated plate

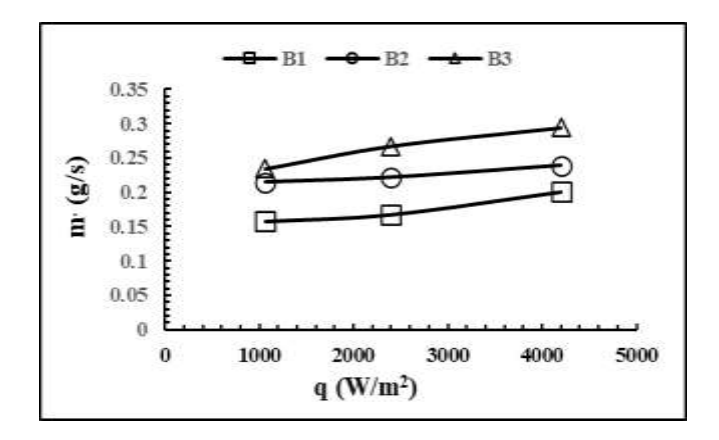


Figure 5. Variation of mass flow rate versus heat flux on two sides of a heated plate

4.2 Experimental convection heat transfer coefficient

Figures 6 and 7 illustrate that the convection heat transfer coefficient increases with Reynolds number, which aligns with the classical Nu–Re behavior observed in porous media. During single-plate heating, B1 displayed higher Reynolds numbers at the same heat flux due to its lower porosity, which accelerated local velocities. However, its heat transfer coefficient (ranging from 11.4 to 56.15 W/m²·°C) did not surpass those of B2 (10.93 to 51.52 W/m²·°C) or B3 (10.66 to 49.53 W/m²·°C). This suggests that the limited bulk flow in

B1 outweighed the benefits of its narrower pore dimensions. Under two-sided heating, B1 maintained a relatively stable Reynolds number (940 to 1200), while B2 and B3 experienced significant enhancements, with their coefficients rising to approximately 98.8 W/m²·K and 94 W/m²·K, nearly doubling the values observed during single heating. This improvement is attributed to higher surface temperatures and stronger buoyancy-driven flow. This observation aligns with the findings of Kailash et al. [38], who noted that combining greater surface exposure with enhanced buoyancy promotes convective heat transfer in porous systems.

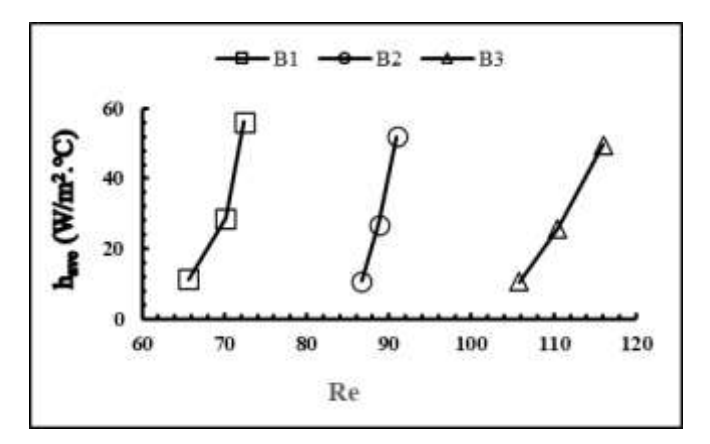


Figure 6. The variation of the convection heat transfer coefficient in relation to the Re number for a heating surface on single side

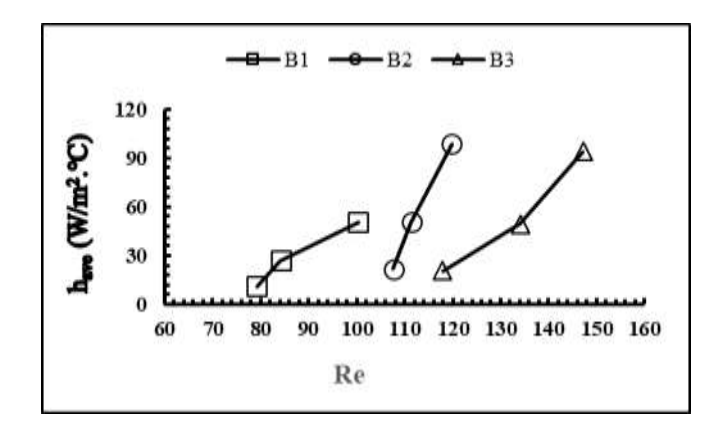


Figure 7. The variation of the convection heat transfer coefficient in relation to the Re number for a heating surface on two parallel sides

4.3 Pressure drop

Figure 8 illustrates that the pressure drop across the porous pad decreases as the sphere diameter increases, which aligns with the Ergun and Forchheimer models. The smallest spheres (B1) experienced the highest pressure drops despite having lower Reynolds numbers; this is attributed to reduced porosity and greater flow resistance. For B1, the pressure drop per pad height ranged from 9.2 to 10.7 Pa/m under single-sided heating and 11.8 to 13.5 Pa/m under double-sided heating. These values represent increases of 33.6% and 45% compared to B2 and B3, respectively. This confirms the hydraulic penalty associated with smaller pore channels, where narrower flow passages lead to intensified viscous and inertial losses. In contrast, the larger spheres (B3) exhibited lower resistance and pressure drops, demonstrating their advantage in reducing pumping power while still maintaining adequate heat transfer

performance. These findings are consistent with those of Ahn et al. [39] and Li and Feng [40].

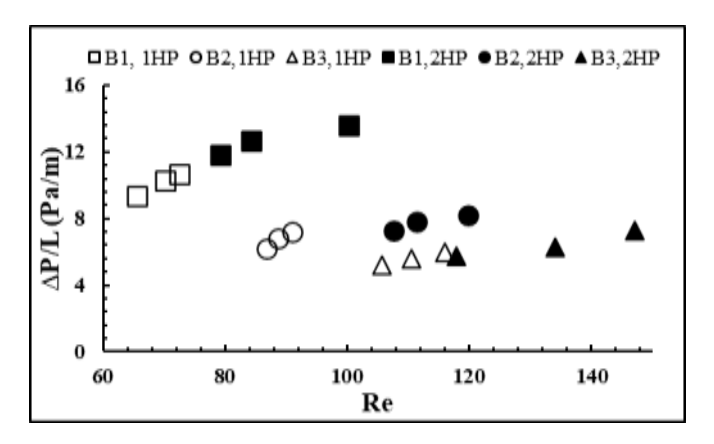


Figure 8. Variation of pressure drop versus Reynolds number across the ball pad with single and two heated plates

5. PRACTICAL IMPLICATIONS

The results reveal an important design trade-off. Smaller spheres enhance surface area and improve heat transfer, but they also lead to a significantly higher-pressure drop, which requires more pumping or fan power. In contrast, larger spheres provide lower flow resistance, making them advantageous in applications where energy efficiency is a priority, even if this means a moderate reduction in heat transfer. For instance, in solar air heaters or compact heat exchangers, smaller spheres may be preferred for maximizing thermal performance. However, in industrial cooling systems, larger spheres might be chosen to reduce operating costs by lowering the pressure drop. Therefore, carefully selecting the size of the spheres allows engineers to balance thermal enhancement with hydraulic efficiency based on the specific requirements of their applications.

6. CONCLUSIONS

This study experimentally examined the thermo-hydraulic performance of glass ball porous pads with varying sphere diameters, under both single-sided and double-sided heating. The results revealed that sphere size has a significant impact on heat transfer and flow resistance due to its effect on porosity. Larger spheres (B3) facilitated increased mass flow and reduced pressure drop, while smaller spheres (B1) resulted in higher Reynolds numbers but also caused greater flow resistance and limited thermal gains. The implementation of two-sided heating substantially enhanced convection, nearly doubling the heat transfer coefficients for spheres B2 and B3 when compared to single-sided heating. Overall, the findings demonstrate the trade-off between thermal enhancement and hydraulic penalties: smaller spheres offer a larger heat transfer surface area but lead to increased pressure drops, whereas larger spheres promote hydraulic efficiency with moderate heat transfer. These outcomes provide valuable insights for selecting packing sizes in porous media applications, such as solar air heaters, cooling devices, and compact heat exchangers, where balancing energy efficiency and thermal performance is crucial.

REFERENCES

- [1] Kakaç, S., Liu, H., Pramuanjaroenkij, A. (2012). Heat Exchanger, Selection, Rating, and Thermal Design. Third Edition: CRC Press.
- [2] Whitaker, S. (1968). Introduction to Fluid Mechanics. New Jersey: Prentice-Hall.
- [3] Pavel, B.I., Mohamad, A.A. (2004). An experimental and numerical study on heat transfer enhancement for gas heat exchangers fitted with porous media. International Journal of Heat and Mass Transfer, 47(23): 4939-4952. https://doi.org/10.1016/j.ijheatmasstransfer.2004.06.014
- [4] Dehghan, M., Valipour, M.S., Saedodin, S. (2016). Microchannels enhanced by porous materials: Heat transfer enhancement or pressure drop increment? Energy Conversion and Management, 110: 22-32. https://doi.org/10.1016/j.enconman.2015.11.052
- [5] Mahmoudi, Y., Maerefat, M. (2011). Analytical investigation of heat transfer enhancement in a channel partially filled with a porous material under local thermal non-equilibrium condition. International Journal of Thermal Sciences, 50(12): 2386-2401. https://doi.org/10.1016/j.ijthermalsci.2011.07.008
- [6] Mahmoudi, Y., Karimi, N. (2014). Numerical investigation of heat transfer enhancement in a pipe partially filled with a porous material under local thermal non-equilibrium condition. International Journal of Heat and Mass Transfer, 68: 161-173. https://doi.org/10.1016/j.ijheatmasstransfer.2013.09.020
- [7] Mohamad, A.A. (2003). Heat transfer enhancements in heat exchangers fitted with porous media Part I: Constant wall temperature. International Journal of Thermal Sciences, 42(4): 385-395. https://doi.org/10.1016/S1290-0729(02)00039-X
- [8] Wang, B., Hong, Y., Hou, X., Xu, Z., Wang, P., Fang, X., Ruan, X. (2015). Numerical configuration design and investigation of heat transfer enhancement in pipes filled with gradient porous materials. Energy Conversion and Management, 105: 206-215. https://doi.org/10.1016/j.enconman.2015.07.064
- [9] Youssif, Y.F., Kadhum, M.H., Ali, A.H. (2020). Experimental study for laminar forced convection heat transfer enhancement from horizontal tube heated with constant heat flux, by using different types of porous media. IOP Conference Series: Materials Science and Engineering, 928(2): 022086. https://doi.org/10.1088/1757-899X/928/2/022086
- [10] Abdulkareem, H.N., Hilal, K.H. (2020). Convection heat transfer analysis in a vertical porous tube. Wasit Journal of Engineering Sciences, 8(1): 31-45. https://doi.org/10.31185/ejuow.Vol8.Iss1.153
- [11] Yousif, M.F., Shehab, S.N., Jaffal, H.M. (2020). Effect of porous media on the performance characteristics of a concentric vertical annular tube. Journal of Advanced Research in Fluid Mechanics and Thermal Sciences, 75(2): 94-112.
- [12] Abbas, M.N. (2011). Modeling of porosity equation for water flow through packed bed of monosize spherical packing. Journal of engineering and Sustainable development, 15(4): 205-226.
- [13] Saleh, A.M., Rasheed, S., Smasem, R. (2018).

 Convection heat transfer in a channel of different cross section filled with porous media. Kufa Journal of Engineering, 9(2): 57-73.

- http://dx.doi.org/10.30572/2018/kje/090205
- [14] Yang, K., Liu, K., Wang, J. (2021). Pore-scale numerical simulation of convection heat transfer in high porosity open-cell metal foam under rotating conditions. Applied Thermal Engineering, 195: 117168. https://doi.org/10.1016/j.applthermaleng.2021.117168
- [15] Yuan, W., Fang, G., Zhang, X., Tang, Y., Wan, Z., Zhang, S. (2018). Heat transfer and friction characteristics of turbulent flow through a circular tube with ball turbulators. Applied Sciences (Switzerland), 8(5): 776. https://doi.org/10.3390/app8050776
- [16] Hilal, K.H., Saleh, A.M., Ebraheem, M.H. (2014). An experimental study on heat transfer enhancement for porous heat exchange in rectangular duct. Engineering and Technology Journal, 32(11): 2788-2802. https://doi.org/10.30684/etj.32.11a.15
- [17] Jiang, P.X., Li, M., Lu, T.J., Yu, L., Ren, Z.P. (2004). Experimental research on convection heat transfer in sintered porous plate channels. International Journal of Heat and Mass Transfer, 47(10-11): 2085-2096. https://doi.org/10.1016/j.ijheatmasstransfer.2003.12.004
- [18] Zhang, H., Chen, L., Liu, Y., Li, Y. (2013). Experimental study on heat transfer performance of lotus-type porous copper heat sink. International Journal of Heat and Mass Transfer, 56(1-2): 172-180. https://doi.org/10.1016/j.ijheatmasstransfer.2012.08.047
- [19] Rasheed, S.A., Hasan, A.J. (2022). Effect of orientation on the natural convection heat transfer from a heated triangular prism embedded in porous media. Case Studies in Thermal Engineering, 35: 102134. https://doi.org/10.1016/j.csite.2022.102134
- [20] Hassan, O.H., Sultan, G.I., Sabry, M.N., Hegazi, A.A. (2022). Investigation of heat transfer and pressure drop in a porous media with internal heat generation. Case Studies in Thermal Engineering, 32: 101849. https://doi.org/10.1016/j.csite.2022.101849
- [21] Salman, A.H.A., Hilal, K.H., Ghadhban, S.A. (2022). Enhancing performance of PV module using water flow through porous media. Case Studies in Thermal Engineering, 34: 102000. https://doi.org/10.1016/j.csite.2022.102000
- [22] Mahdi, S.R., Suhad, A. (2023). Experimental study convection heat transfer inside the triangular duct filled with porous media. Engineering and Technology Journal, 41(1): 203-217. https://doi.org/10.30684/etj.2022.136144.1297
- [23] Ali, S.A., Rasheed, S.A. (2024). Experimental investigation of forced convection in plain or partly inserted square channel with porous media. Journal of Engineering, 30(4): 99-117. https://doi.org/10.31026/j.eng.2024.04.07
- [24] Boulhidja, S., Bourouis, A., Boukelia, T.E., Omara, A. (2024). Mixed convection air-cooled PV/T solar collector with integrate porous medium. Journal of the Brazilian Society of Mechanical Sciences and Engineering, 46(3): 144. https://doi.org/10.1007/s40430-024-04728-x
- [25] Saihood, R.G., Ala, M.F.F. (2024). Experimental study of partial open side effect on natural convection in a porous cavity. Journal of Engineering, 30(6): 172-187. https://doi.org/10.31026/j.eng.2024.06.11
- [26] Xiang, J., Chen, K., Jiang, W., Tang, A., Jin, Y., Ding, H., Cai, T. (2025). Experimental investigation of flow and heat transfer characteristics in single-tube liquid-

- solid fluidized bed heat exchangers. http://doi.org/10.2139/ssrn.5370938
- [27] Bavandla, K.C., Srinivasan, V. (2024). Rayleigh–Bènard convection in a gas-saturated porous medium at low Darcy numbers. ASME Journal of Heat and Mass Transfer, 146(5): 051001. https://doi.org/10.1115/1.4064327
- [28] Karra, S.K., Apte, S.V. (2024). Numerical investigation of turbulent flow over a randomly packed sediment bed using a variable porosity continuum model. Physics of Fluids, 36(11): 115177. https://doi.org/10.1063/5.0237201
- [29] Lee, H., Gossler, M., Zosseder, K., Blum, P., Bayer, P., Rau, G.C. (2025). Laboratory heat transport experiments reveal grain-size-and flow-velocity-dependent local thermal non-equilibrium effects. Hydrology and Earth System Sciences, 29(5): 1359-1378. https://doi.org/10.5194/hess-29-1359-2025
- [30] Bansal, A.K. (2025). Enhancing heat transfer in fluidized bed reactors using iron oxide-coated glass beads. SGS-Engineering & Sciences, 1(2).
- [31] Singh, D., Goswami, R., Mishra, P., Kumar, V., Mishra, I.M. (2025). Heat transfer characteristics in a liquid-solids fluidisation bed: Effect of particle diameter and fluids. Powder Technology, 460: 121013. https://doi.org/10.1016/j.powtec.2025.121013
- [32] Zhang, H., Gong, Y., Li, Y., Ma, H., He, J., Jiang, W. (2025). An array photocatalytic reactor based on porous glass bead with loaded zirconia photocatalyst for degradation of rhodamine B in dye wastewater. Journal of Water Process Engineering, 69: 106789. https://doi.org/10.1016/j.jwpe.2024.106789
- [33] Zhang, Y., Sufian, A., Scheuermann, A. (2025). Observations on the steady-state fluidised bed porosity at low Reynolds numbers. Powder Technology, 457: 120864. https://doi.org/10.1016/j.powtec.2025.120864
- [34] Sheppard, J., Chen, R.H., Lan, Y., Ma, R. (2025). Freeze casting of porous copper with lamellar morphology from cupric oxide suspensions for enhancing through-plane thermal conductivity. International Journal of Thermophysics, 46(8): 109. https://doi.org/10.1007/s10765-025-03578-6
- [35] Hilal, K.H., Ghadhban, S.A., Aun, S.H.A. (2025). Experimental study of heat transfer to air flowing through an inclined porous duct. Pollack Periodica. https://doi.org/10.1556/606.2025.01242
- [36] Saqar, T.I., Ahmed, O.K., Alomar, O.R., Algburi, S. (2025). Performance of double-pass storage solar air heater using two types of porous media and fin plate. Energy Storage, 7(4): e70167. https://doi.org/10.1002/est2.70167
- [37] Holman, J.P. (2013). Heat Transfer. 10th Edition, Higher Education, The Mc Hill Companies.
- [38] Kailash, O., Choudhary Bishwajeet, N.K., Gajera Umang, B., PrajapatSumit, B., Karangiya Gopal, A. (2015). Design and experimental analysis of pipe in pipe heat exchanger. International Journal of Modern Engineering Research (IJMER), 5(3): 42-48.
- [39] Ahn, H.H., Moon, J.Y., Chung, B.J. (2022). Influences of sphere diameter and bed height on the natural convection heat transfer of packed beds. International Journal of Heat and Mass Transfer, 194: 123032. https://doi.org/10.1016/J.IJHEATMASSTRANSFER.20 22.123032

[40] Li, N., Feng, P. (2025). Flow and heat transfer		∞ T	Ambient temperature (°C)	
characteristics in randomly packed beds with small D/d		T_b	Bulk temperature (°C)	
ratios. Numerical Heat Transfer, Part A: Applications,		T_{s}	Outside surface of test rig temperature (°C)	
86(14): 4860-4879.		T_{w}	Hot surface temperature (°C)	
https://doi.org/10.1080/10407782.2024.2324069		V_b	Total volume (water + glass ball) (m ³)	
-		$ m V_w$	Water volume (m ³)	
		Q	Net heat transfer rate (W)	
NOMENCLATURE		q_{in}	Input heat transfer to the porous pad (W)	
		q_o	Heat loss to the ambient (W)	
A_p	Plate area (m ²)	q_r	Heat loss by radiation to the ambient (W)	
A_{o}	Outside area (m ²)	σ	Stefan-Boltzmann constant 5.669 × 10 ⁸	
I	Electric current (A)		$(W/m^2 \cdot K^4)$	
h_{ave}	Average convection heat transfer	ϵ	Emissivity	
	coefficient (W/m ² ·°C)	3	Porosity	
h_o	Outside surface of test rig convection heat	1HP	Single heating plate	
	transfer convection (W/m ² .°C)	2HP	Two parallel heating plates	
P_{ele}	Electric power (W)		-	